Article

Discovery Medicine 2026; 38(209): 1788–1801
https://doi.org/10.24976/Discov.Med.202638209.139

Lin28b Overexpression Enhances Facial Nerve Regeneration and Functional Recovery Through AKT/mTOR Signaling Pathway Activation in Mice

Xiaoyan Guo[1,2,3], Qin Hu[4], Qi Lu[1,2,3], Kun Li[1,2,3], Shiming Yang[1,2,3], Weidong Shen[1,2,3,*]

[1]Senior Department of Otolaryngology Head and Neck Surgery, the 6th Medical Center of Chinese PLA General Hospital & Chinese PLA Medical School, 100853 Beijing, China
[2]National Clinical Research Center for Otolaryngologic Diseases, 100853 Beijing, China
[3]State Key Laboratory of Hearing and Balance Science, 100853 Beijing, China
[4]Frontier Institute of Science and Technology, Xi'an Jiaotong University, 710115 Xi'an, Shaanxi, China
*Correspondence: shenweidong@301hospital.com.cn (Weidong Shen)
Submitted: 9 March 2026 Revised: 20 April 2026 Accepted: 23 April 2026 Published: 20 June 2026

Background: Limited axonal regeneration in mature neurons hinders functional recovery after neural injury. This study aimed to investigate the conserved regulator Lin28, which governs pluripotency-to-differentiation transitions, and to elucidate its role and underlying mechanisms in post-injury neural repair within the facial motor nucleus.

Methods: Using C57BL/6J wild-type mice, human Lin28b-inducible overexpression transgenic mice (*iLIN28B*), and reverse tetracycline-controlled transactivator (rtTA)-only transgenic controls, we established a facial nerve crush injury model (FNI). Quantitative reverse transcription polymerase chain reaction (qRT-PCR), Western blotting, and immunofluorescence were employed to systematically analyze Lin28's roles in facial nerve development and injury repair.

Results: In wild-type mice, Lin28a/b were highly expressed in the facial nucleus during embryonic stages but significantly declined postnatally. On day 3 post-FNI, Lin28a/b expression was significantly upregulated while let-7a/b microRNAs were downregulated. In *iLIN28B* mice, Lin28b overexpression promoted facial motor functional recovery and axonal regeneration at 3 days post-FNI. Moreover, Lin28b overexpression significantly downregulated let-7 microRNA levels and enhanced phosphorylation of protein kinase B (Akt) at Ser473 (pAkt) and ribosomal protein S6 at Ser235/236 (pS6) in the facial nucleus.

Conclusions: Collectively, these findings suggest that Lin28b promotes axonal regeneration following facial nerve injury by downregulating the let-7 microRNAs, while the phosphatidylinositol 3-kinase (PI3K)-AKT-mammalian target of rapamycin (mTOR) pathway mediates, at least in part, the pro-regenerative effect of Lin28b. This study identifies Lin28b as a novel regulator of facial nerve injury repair, highlighting its potential as a molecular therapeutic target for motor nerve regeneration.

Keywords: facial nerve; injury; Lin28; let-7; axonal regeneration

Introduction

The management of peripheral facial paralysis primarily relies on pharmacological interventions and surgical procedures [1]. Although idiopathic facial paralysis usually has a good prognosis, facial paralysis caused by other etiologies (such as infection, tumor, or iatrogenic injury) often results in persistent functional impairments despite prompt treatment [2]. Denervation of facial mimetic muscles results in disfigurement, masticatory dysfunction, and speech impairment, which not only severely compromise quality of life but also predispose patients to psychological comorbidities such as anxiety and depression [3]. Functional recovery is constrained by the poor intrinsic regenerative capacity of mature neurons, resulting from terminal differentiation and developmental silencing of regeneration-promoting pathways, which synergistically impede post-injury repair [4].

Several cell-autonomous molecular regulators, such as Krüppel-like factors (KLFs) and the proto-oncogene c-Myc, have been identified as critical reprogramming factors capable of reversing the terminally differentiated state of somatic cells into induced pluripotent stem cells (iPSCs), which subsequently demonstrate an indirect modulatory effect on neuronal growth potential [5,6]. Lin28 RNA-binding protein, initially identified in Caenorhabditis elegans, has been demonstrated to significantly enhance the reprogramming efficiency of human somatic cells into iPSCs [7]. As two paralogs in vertebrates, Lin28a and Lin28b play vital roles in growth-related processes, including body size regulation, puberty control [8], glucose metabolism [9], and tissue regeneration [10]. Their functional mechanisms primarily rely on post-transcriptional inhibition of the let-7 microRNA (miRNA) family, blocking the biosynthesis of mature let-7 miRNAs [11]. In *C. elegans*, Lin28 regulates

early cell proliferation independently of let-7 and promotes later cell differentiation by suppressing let-7 [12]. In zebrafish, following retinal injury, reactivation of Lin28 plays a critical role in the dedifferentiation of Müller glia, their re-entry into the cell cycle to generate new neurons, and the regulation of regeneration-associated gene expression [10]. Importantly, in mouse models, studies have demonstrated that activation of Lin28a in the retina significantly enhances axonal regenerative capacity following optic nerve injury [13]. This effect may involve modulation of presynaptic inhibitory neuronal function, thereby indirectly promoting the survival and regeneration of retinal ganglion cells (RGCs) [14]. However, the spatiotemporal expression patterns of Lin28a/b in the facial nucleus of the brainstem and their functional roles in regulating axonal regeneration following facial nerve injury remain largely unexplored.

The phosphatidylinositol 3-kinase (PI3K)/protein kinase B (Akt)/mammalian target of rapamycin (mTOR) pathway serves as a core intracellular regulatory network and is extensively involved in cell growth, proliferation, and differentiation [15–17]. This pathway has been confirmed to play multiple critical roles in peripheral nerve injury repair [18–21]. For instance, in sciatic nerve injury models, activation of the Akt-mTOR signaling promotes axonal regeneration and functional recovery [22]. However, the role of this signaling pathway in axonal regeneration following facial nerve injury currently has not yet been systematically investigated.

This study is the first to elucidate the critical role of the Lin28 signaling axis in facial nerve injury repair. Experimental validation using a transgenic mouse model demonstrated that overexpression of Lin28b significantly enhances motor functional recovery and axon regeneration post-injury, an effect that may be partially mediated by the PI3K/AKT/mTOR pathway. These findings establish Lin28b as a novel molecular candidate for targeted therapeutic strategies in motor neuron injury.

Materials and Methods

Experimental Animals

All animal procedures were approved by the Animal Ethics Committee of the Chinese PLA General Hospital (Approval No.2020-X16-50). For this study, we employed three mouse models: (1) C57BL/6J wild-type mice, purchased from Spaford (Beijing) Biotechnology Co., Ltd., were used to map the spatiotemporal expression profiles of Lin28a/b in the primary motor cortex and facial nucleus during development and post-facial nerve injury. Three independent experiments were performed for each condition, with three mice per experiment; (2) Human Lin28b conditional overexpression transgenic mice (*iLIN28B*): This strain carries the human Lin28b transgene inserted downstream of the Gt(Rosa26)Sor promoter, enabling tetracycline-inducible overexpression via the reverse tetracycline-controlled transactivator (rtTA) system, with transcriptional activation requiring doxycycline (dox; Cat. No. D5207, Sigma-Aldrich Co., LLC, St. Louis, MO, USA) administration; and (3) rtTA-only transgenic control mice (M2rtTA): to control for potential confounding effects of the tetracycline-inducible transgene activation system. Both strains were generously provided by Prof. Xiaojun Li's research group at Xi'an Jiaotong University. Male M2rtTA$^{tg/tg}$ mice were crossed with female Lin28b$^{tg/+}$ mice to generate M2rtTA$^{tg/+}$; Lin28b$^{tg/+}$ mice and M2rtTA$^{tg/+}$ mice, which were used as *iLIN28B* mice and M2rtTA control mice in experiments, respectively. To investigate the effects of Lin28b overexpression on axon regeneration following facial nerve injury, 2-week-old *iLIN28B* mice (n = 6) and their littermate M2rtTA controls (n = 6) were used. In addition, *iLIN28B* mice (n = 3) and their littermate M2rtTA control mice (n = 3) were used to detect the expression levels of LIN28B-related proteins in the primary motor cortex and facial nucleus, as well as the expression levels of let-7 miRNAs in the facial nucleus. All surgical procedures were performed under anesthesia induced by intraperitoneal injection of tribromoethanol (200 mg/kg). At the experimental endpoint, mice were humanely euthanized by carbon dioxide inhalation followed by cervical dislocation, and tissues were subsequently collected for analysis.

Development and Functional Evaluation of a Facial Nerve Crush Injury Model

Mice were anesthetized via intraperitoneal (i.p.) injection of tribromoethanol (200 mg/kg). 2,2,2-Tribromoethanol (≥98.0%, GC) was purchased from Shanghai Aladdin Biochemical Technology Co., Ltd. (Cat. No. T161626, Aladdin, Shanghai, China). Under microscopic guidance, the left extracranial facial nerve was surgically exposed. A standardized facial nerve crush injury (FNI) was induced by clamping the main trunk approximately 0.3 cm distal to the stylomastoid foramen using Dumont #5/45 vascular forceps (Dumont SA, Montignez, Canton of Jura, Switzerland) for 30 seconds. Postoperatively, mice were monitored daily for general condition. Facial nerve functional recovery was evaluated at postoperative days 1 and 3 using the Simone 10-point scale [23], which quantifies deficits from 0 (complete paralysis) to 10 (normal function; **Supplementary Tables 1,2**). All behavioral assessments were performed in a blinded manner, with investigators unaware of the group assignments for each mouse during scoring. Mice with scores ≤3 points were deemed successful FNI models and included in subsequent analyses.

Quantitative Real-Time PCR

Total RNA was extracted from tissue samples using the miRNeasy Mini Kit (Spin Column) (Cat. No. RC201-01, Vazyme, Nanjing, China). For mRNA expres-

sion analysis, first-strand cDNA was synthesized with the HiScript II Reverse Transcriptase Kit (Cat. No. R323-01, Vazyme, Nanjing, China), followed by quantitative real-time polymerase chain reaction (qRT-PCR) using Fast SYBR Green Master Mix (Cat. No. AG11733, Accurate Biology, Changsha, China) and gene-specific primers. miRNA expression profiling was performed using the stem-loop method: reverse transcription was conducted with the miRNA 1st Strand cDNA Synthesis Kit (Cat. No. MR101-01, Vazyme, Nanjing, China), followed by qRT-PCR amplification with miRNA-specific primers and Unimodal SYBR qPCR Master Mix (Cat. No. MQ102-01, Vazyme, Nanjing, China). Relative expression levels were calculated via the $2^{-\Delta\Delta CT}$ method, with Rpl19 and Rnu6 serving as endogenous controls for mRNA and miRNA normalization, respectively. The primers for Rnu6b were obtained from the Vazyme MQ102-01 kit, and the other primer sequences were adopted as previously described in reference [22] and are listed in **Supplementary Table 3**. All primers were synthesized by Sangon Biotech (Shanghai) Co., Ltd., Shanghai, China.

Western Blot Analysis

Protein samples were extracted from the primary motor cortex and brainstem facial nucleus tissues using RIPA lysis buffer supplemented with protease inhibitor cocktail (Cat. No. P8340, Sigma-Aldrich, St. Louis, MO, USA) and phosphatase inhibitor cocktail (Cat. No. P0044, Sigma-Aldrich, St. Louis, MO, USA). Total protein concentration was measured with a BCA Protein Assay Kit (Cat. No. P0012S, Beyotime Biotechnology, Shanghai, China) following the manufacturer's protocol. Subsequently, an equal amount of protein was loaded into each lane. Each lane of the SDS-PAGE gel was loaded with 20 µg of denatured total protein for electrophoresis and subsequent immunoblotting. After blocking with 5% non-fat milk for 30 min at room temperature, the membranes were incubated overnight at 4 °C with the following primary antibodies: anti-Lin28b (1:1000; Cell Signaling Technology, Cat No. 4196), anti-pS6 Ser235/236 (1:2000; Cell Signaling Technology, Cat No. 2211), anti-pAkt Ser473 (1:2000; Cell Signaling Technology, Cat No. 4060), and anti-β-actin (1:1000, Cell Signaling Technology, Cat. No. 4970). On the following day, the membranes were incubated with HRP-conjugated Goat Anti-Rabbit IgG H&L secondary antibody (Abcam, Cat. No. ab205718) for 1 h at room temperature. After each antibody incubation step, membranes were washed three times with TBST (15 min per wash). Protein bands were visualized using enhanced chemiluminescence and quantified by densitometry analysis with ImageJ software (National Institutes of Health, Bethesda, MD, USA). The gray values of target protein bands and corresponding β-actin reference bands were measured to calculate the relative expression levels of target proteins. The relative expression in experimental groups was presented as fold changes relative to the control group. All statistical analyses were performed using normalized gray values from at least three independent repeated experiments.

Primary Cell Cultures

The facial nucleus from the brainstem was dissected from 2-week-old wild-type and *iLIN28B* mice. The tissue fragments were digested in a solution containing 40 U/mL papain (Cat. No. P4762, Sigma-Aldrich, St. Louis, MO, USA) and 50 U/mL DNase I (Cat. No. AMPD1, Sigma-Aldrich, St. Louis, MO, USA) at 37 °C for 20 minutes, followed by three washes with HBSS. The digested tissues were then mechanically dissociated into single cells in MEM medium (Cat. No. 11095-080, Thermo Fisher Scientific, Waltham, MA, USA) supplemented with B27 (Cat. No. 17504044, Thermo Fisher Scientific, Waltham, MA, USA), L-Glutamax (Cat. No. 35050061, Thermo Fisher Scientific, Waltham, MA, USA), and 1× penicillin/streptomycin (Cat. No. 15140122, Thermo Fisher Scientific, Waltham, MA, USA). The resulting cell suspension was filtered through a 100 µm cell strainer and centrifuged at 800 rpm for 6 minutes. The cell pellet was resuspended in an appropriate amount of the pre-warmed culture medium mentioned above and seeded onto glass coverslips pre-coated with a mixture of 100 µg/mL poly-D-lysine (Cat. No. P7280, Sigma-Aldrich, St. Louis, MO, USA) and 10 µg/mL laminin (Cat. No. 23017015, Thermo Fisher Scientific, Waltham, MA, USA). Under an inverted microscope (Model: IX53, Olympus Corporation, Shinjuku City, Tokyo, Japan), the isolated primary facial nucleus motor neurons exhibited typical neuronal morphology, including bright refractive cell bodies, extended neurites, and a dense interconnected neural network. The cells were subsequently cultured for 3 days. During cell culture, mycoplasma contamination was routinely detected using a PCR-based mycoplasma detection kit (Cat. No. C0301S, Beyotime Biotechnology, Shanghai, China), and all cell cultures used in this study were mycoplasma-negative.

Immunofluorescence

Following fixation with 4% PFA, facial nerve tissues and 3-day cultured neurons were subjected to immunofluorescence staining. Both tissue sections and cultured neurons were blocked in PBS containing 1% BSA and 0.3% Triton X-100, and then incubated overnight at 4 °C with primary antibodies: anti-NF200 (BioLegend, Cat. No. 801701) for tissue sections and anti-Tuj1 (BioLegend, Cat. No.801201) for cultured neurons. Subsequently, all samples were incubated with corresponding Alexa Fluor-conjugated secondary antibodies (Thermo Fisher Scientific, Cat. No. A-11001 and A-11004) for 1 hour at room temperature. Thorough washing with PBST was performed after each antibody incubation step. Finally, the samples were mounted with Fluoroshield mounting medium (Cat. No. F6182, Sigma-Aldrich, St. Louis, MO, USA) and imaged using an

inverted fluorescence microscope (Model: IX73, Olympus Corporation, Shinjuku City, Tokyo, Japan). Axon quantification was performed using Image J (Version 1.54f, National Institutes of Health, Bethesda, MD, USA). Regions of interest (ROIs) covering the full nerve diameter were defined perpendicular to the nerve axis at 200 µm and 500 µm distal to the injury site. NF200-labeled axons were identified using a constant threshold, and the "Analyze Particles" function was used to automatically quantify axonal profiles. Three non-consecutive sections per animal (n = 6 per group) were quantified by an observer blinded to the experimental groups. Similarly, the length of facial neuron processes in each group was measured using ImageJ software. Thirty β-tubulin-positive neurons per group were randomly selected in a zigzag pattern across the visual fields, and the longest process length of each neuron was taken as the final statistical length, which was quantified by an observer blinded to the experimental groups.

Statistical Analyses

Statistical analyses were performed using GraphPad Prism 10 (GraphPad Software, LLC, San Diego, CA, USA), with significance set at $p < 0.05$. All qPCR and Western blot data were normalized to the control group and expressed as fold change relative to the control. Data are presented as mean ± standard error of the mean (SEM) unless otherwise specified. Prior to statistical analysis, normality was assessed using the Shapiro-Wilk test, and homogeneity of variances was evaluated using the Brown-Forsythe test; these tests were performed using GraphPad Prism 10. For data meeting the assumptions of normality and equal variance, parametric tests were applied. For two-group comparisons, one-sample *t*-tests (hypothetical mean = 1) were used for normalized relative data, while unpaired two-tailed Student's *t*-tests were applied for non-normalized comparisons. For comparisons among three or more groups, one-way analysis of variance (ANOVA) followed by Tukey's multiple comparison test was used to determine the statistical significance.

Full statistical details (tests, exact n values, replication definitions) are provided in figure legends.

Results

Lin28a/b may be Involved in the Early Development of the Facial Nerve

First, we systematically analyze the expression levels of Lin28a/b in the primary motor cortex and facial nucleus of the brainstem in wild-type mice at embryonic days 10.5 (E10.5), E12.5, E14.5, E16, E17, E18, postnatal days 0 (P0), P3, P7, and P14. The results of qRT-PCR showed that the mRNA levels of Lin28a/b exhibited dynamic changes during development. In the primary motor cortex, compared with those at E10.5, the mRNA levels of Lin28a/b significantly decreased at E14.5 ($p < 0.05$), further declined at E16 ($p < 0.001$), and remained at low levels during subsequent developmental stages (Fig. 1A,B). In the facial nucleus, the mRNA levels of Lin28a/b remained relatively stable during embryonic development after E10.5, then significantly decreased on the day of birth (P0) ($p < 0.01$), and persisted at low levels postnatally (Fig. 1C,D). These temporal expression patterns suggest that Lin28a/b may play an important role in regulating the early development of the facial nerve.

Lin28/let-7 Axis Activation in the Facial Nucleus Following Nerve Injury

To investigate whether the expression of Lin28a/b in the facial nucleus responds to facial nerve injury, we established a left extracranial FNI in 2-week-old wild-type mice, with sham-operated groups (Sham) as controls. Facial nucleus tissues were collected at 1, 3, and 7 days post-FNI. Quantitative analysis demonstrated that compared to the Sham group, the mRNA levels of Lin28a/b in the FNI group began to upregulate at 1-day post-FNI ($p < 0.05$), peaked at 3 days ($p < 0.001$), and returned to baseline levels by 7 days (Fig. 2A,B). Notably, this upregulation was accompanied by significant downregulation of let-7a/b at 3 days post-FNI (Fig. 2C,D, $p < 0.001$ for let-7a, $p = 0.01$ for let-7b). To further elucidate the regulatory relationship between Lin28a/b and the let-7 miRNA family following facial nerve injury, we collected facial nucleus tissues immediately after FNI (0 h) and at 3 h, 6 h, 12 h, and 24 h post-FNI, and then detected the levels of Lin28a/b mRNAs and let-7a/b. The results showed that within 24 hours after FNI, the levels of Lin28a/b mRNAs were significantly upregulated, while let-7a and let-7b remained at the baseline during this period (Fig. 2E,F, $p = 0.013$ for Lin28a, $p < 0.022$ for Lin28b, $p = 0.147$ for let-7a, $p = 0.165$ for let-7b). Collectively, these findings suggest that the upregulation of Lin28a/b in the facial nucleus after facial nerve injury may precede or occur independently of let-7 downregulation, supporting a potential upstream role of Lin28a/b in regulating axonal regeneration.

Overexpression of Lin28b in the Facial Nucleus Suppresses let-7 miRNA Levels

To validate the efficacy of doxycycline-induced LIN28B overexpression and its impact on let-7 miRNAs regulation, we treated *iLIN28B* transgenic mice and their control littermates with doxycycline (2 mg/mL in drinking water) *ad libitum* for two consecutive days. Tissue samples from the primary motor cortex and facial nucleus were harvested 48 hours post-treatment. Following normalization to the control group, Western blot analysis revealed a significant increase in LIN28B protein levels in both the primary motor cortex ($p = 0.008$) and facial nucleus ($p = 0.048$) of *iLIN28B* mice compared to controls (Fig. 3A,B). Concurrently, let-7 miRNA levels (excluding let-7c, which remained unaltered) were

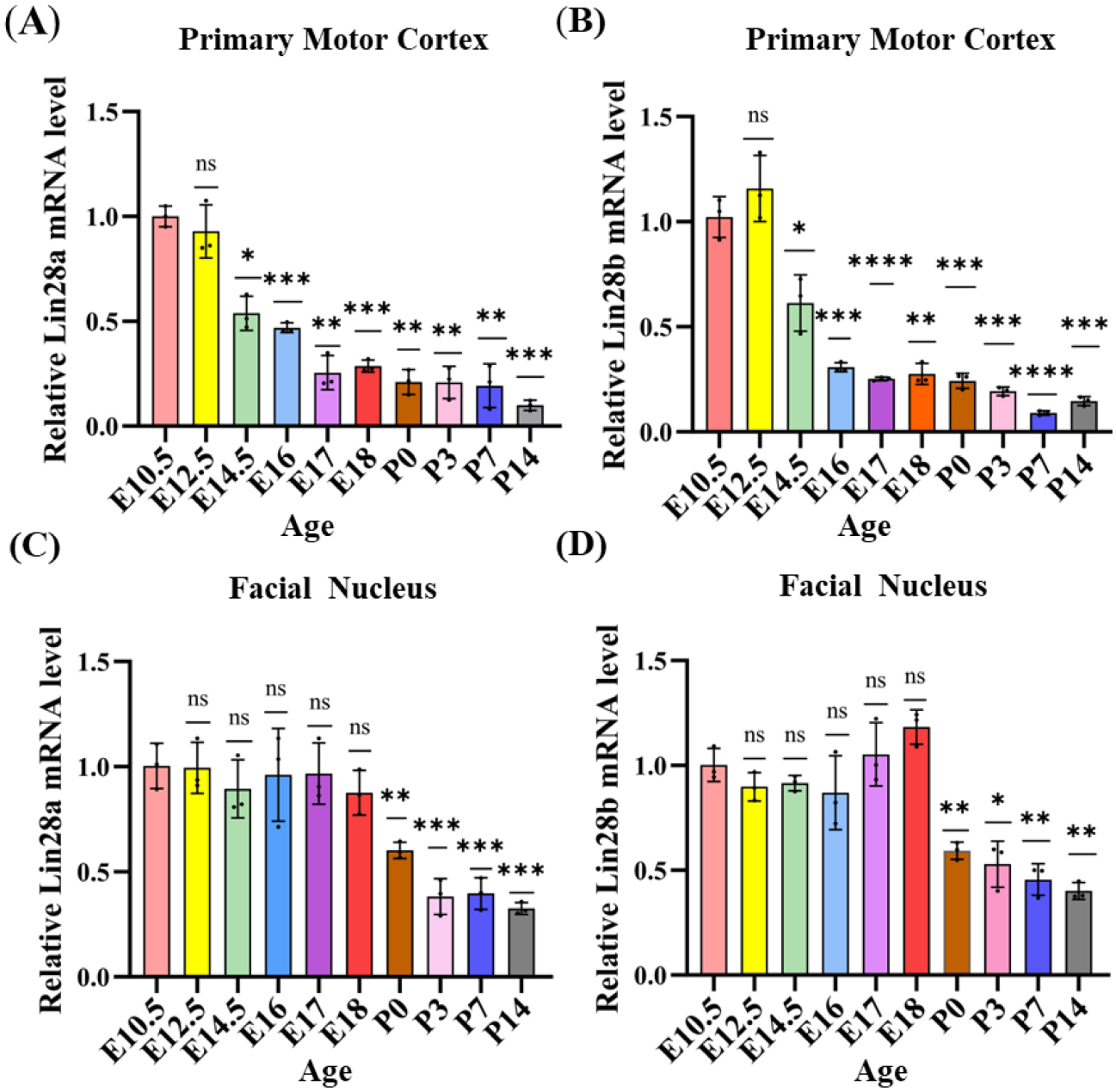

Fig. 1. The expression profiles of Lin28a/b in the primary motor cortex and the facial nucleus during mouse development. (A,B) qRT-PCR analysis revealed that mRNA levels of Lin28a (A) and Lin28b (B) in the mouse primary motor cortex progressively declined from embryonic day 10.5 (E10.5) to embryonic day 14.5 (E14.5), stabilizing at basal levels thereafter (post-E16). (C,D) Lin28a (C) and Lin28b (D) mRNA levels in the facial nucleus remained stable during embryonic development, decreased sharply at P0, and stayed low after birth. Data are expressed as mean ± SEM. Statistical comparisons were performed relative to the E10.5 group as the reference control. One-way ANOVA followed by Tukey's multiple comparisons test; $^{*}p < 0.05$, $^{**}p < 0.01$, $^{***}p < 0.001$, $^{****}p < 0.0001$; ns, not significant. n = 3 independent experiments. qRT-PCR, Quantitative reverse transcription polymerase chain reaction; SEM, standard error of the mean; ANOVA, analysis of variance.

markedly reduced in the facial nucleus of *iLIN28B* mice (Fig. 3C). The *p* values were 0.002, 0.030, 0.074, 0.006, 0.013, 0.002, <0.0001, and 0.002 for let-7a, let-7b, let-7c, let-7d, let-7e, let-7f, let-7g, and let-7i, respectively. These findings align with the established role of Lin28a/b in suppressing mature let-7 biogenesis.

Lin28b Overexpression Facilitates Facial Nerve Functional Recovery and Enhances Axon Regeneration

To investigate whether overexpression of Lin28b promotes nerve regeneration following facial nerve injury. On the 3rd day of dox treatment, the facial nerve crush in-

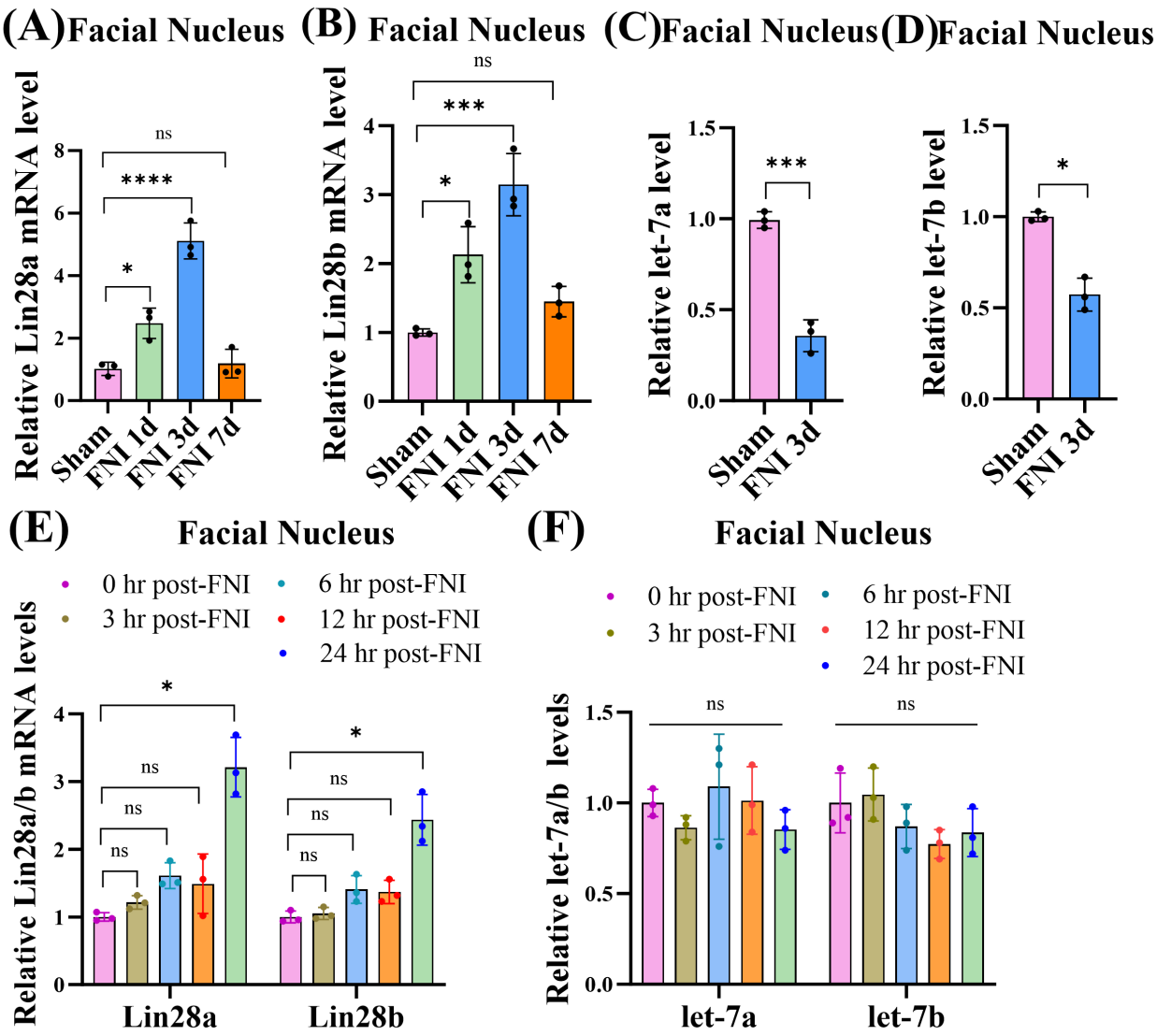

Fig. 2. Lin28/let-7 axis activation in the facial nucleus following nerve injury. (A,B) qRT-PCR analysis demonstrated that facial nerve injury (FNI) significantly upregulated Lin28a (A) and Lin28b mRNA (B) levels in the facial nucleus compared to the Sham group. Statistical analyses were performed using one-way ANOVA followed by Tukey's multiple comparisons test. (C,D) FNI significantly downregulated let-7a (C) and let-7b (D) levels in the facial nucleus. Comparisons between Sham and FNI groups were conducted using unpaired two-tailed Student's *t*-tests. (E,F) The increase of Lin28a/b mRNA levels occurred within 12–24 h after FNI, whereas no significant change in let-7a or let-7b levels was observed within 24 h after FNI. One-way ANOVA followed by Tukey's multiple comparisons test was used for these analyses. The color of each bar in (A–D) matches the color of the corresponding data point. Group classification is based on the color of the individual data points in (E–F). Data are expressed as mean ± SEM. $^{*}p < 0.05$, $^{***}p < 0.001$, $^{****}p < 0.0001$; ns, not significant, n = 3 independent experiments.

jury was performed. Facial nerve function was then assessed using the Simone 10-point scoring scale on the 1st and 3rd days after FNI. The results showed that on day 1 post-FNI, the facial nerve function scores were 2.17 ± 0.167 in the control mice and 2.67 ± 0.211 in the *iLIN28B* mice, with no significant intergroup difference ($p = 0.094$; Fig. 4A). Both scores were below the established threshold for successful model induction (≤3 points), indicating robust establishment of the FNI model [23]. By day 3 post-FNI, scores in *iLIN28B* mice significantly increased to 4.00 ± 0.894, compared to 2.67 ± 0.516 in control mice ($p = 0.013$; Fig. 4A). Based on the aforementioned findings, which demonstrated that the spontaneous upregulation of Lin28a and Lin28b triggered by facial nerve injury was markedly robust by day 3 post-FNI (Fig. 2A,B), we collected approximately 1 cm of facial nerve tissue en-

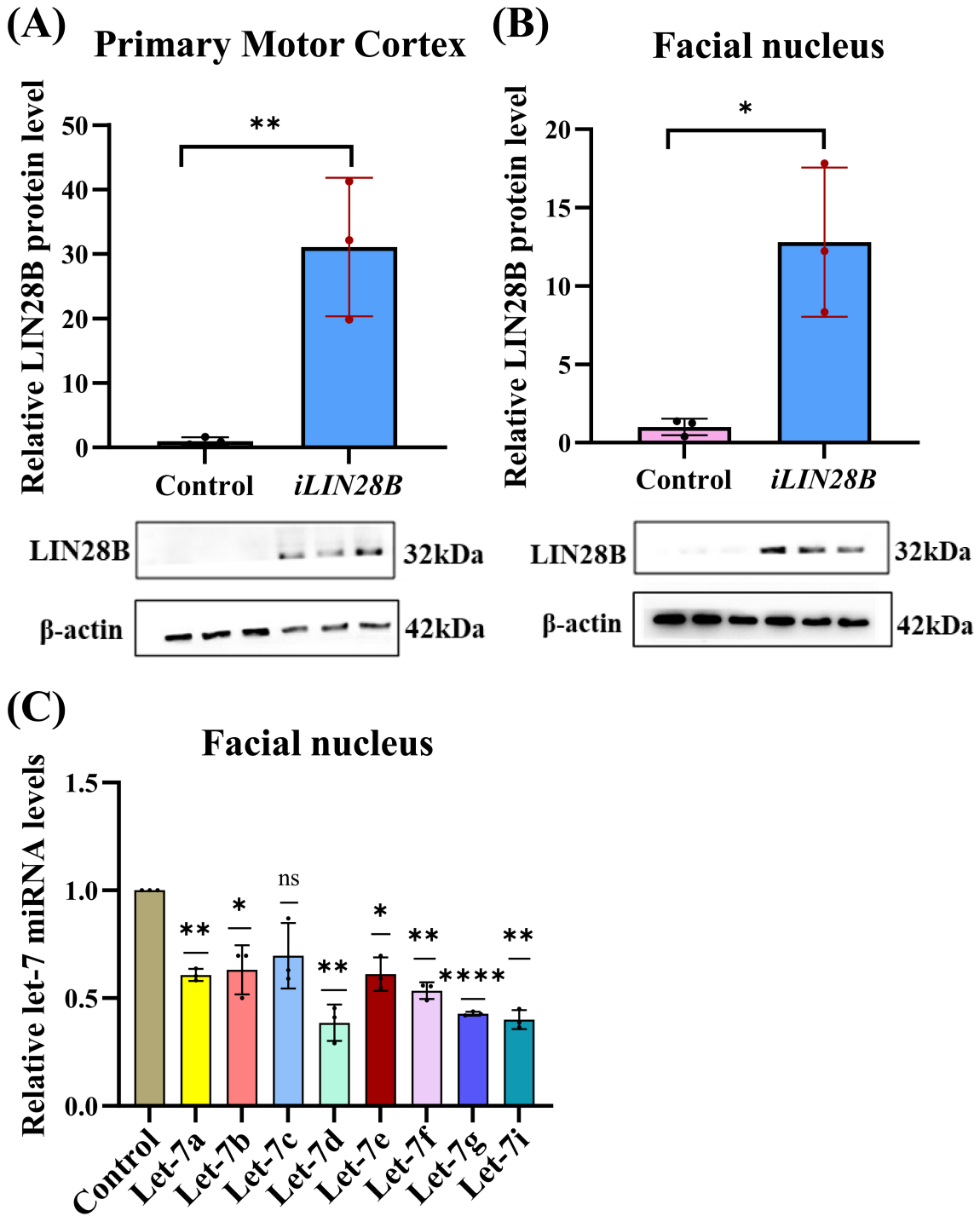

Fig. 3. Two-day dox induction in *iLIN28B* mice upregulated LIN28B protein and downregulated let-7 miRNAs in the primary motor cortex and facial nucleus. (A,B) LIN28B protein was detected by Western blotting in the primary motor cortex (A) and facial nucleus (B) of *iLIN28B* mice, confirming its upregulation. (C) qRT-PCR analysis showed that the levels of let-7 miRNAs in the facial nerve nucleus of *iLIN28B* mice significantly decreased (n = 3 independent experiments). Data are expressed as mean ± SEM. One sample *t*-test; ns, not significant. $^{*}p < 0.05$, $^{**}p < 0.01$, $^{****}p < 0.0001$ compared with the control if not designated. n = 3 independent experiments.

compassing the injury site on day 3 post-FNI after functional assessments. Quantitative immunofluorescence analysis revealed that the axon count in the *iLIN28B* group at 200 µm distal to the facial nerve crush injury site was sig-

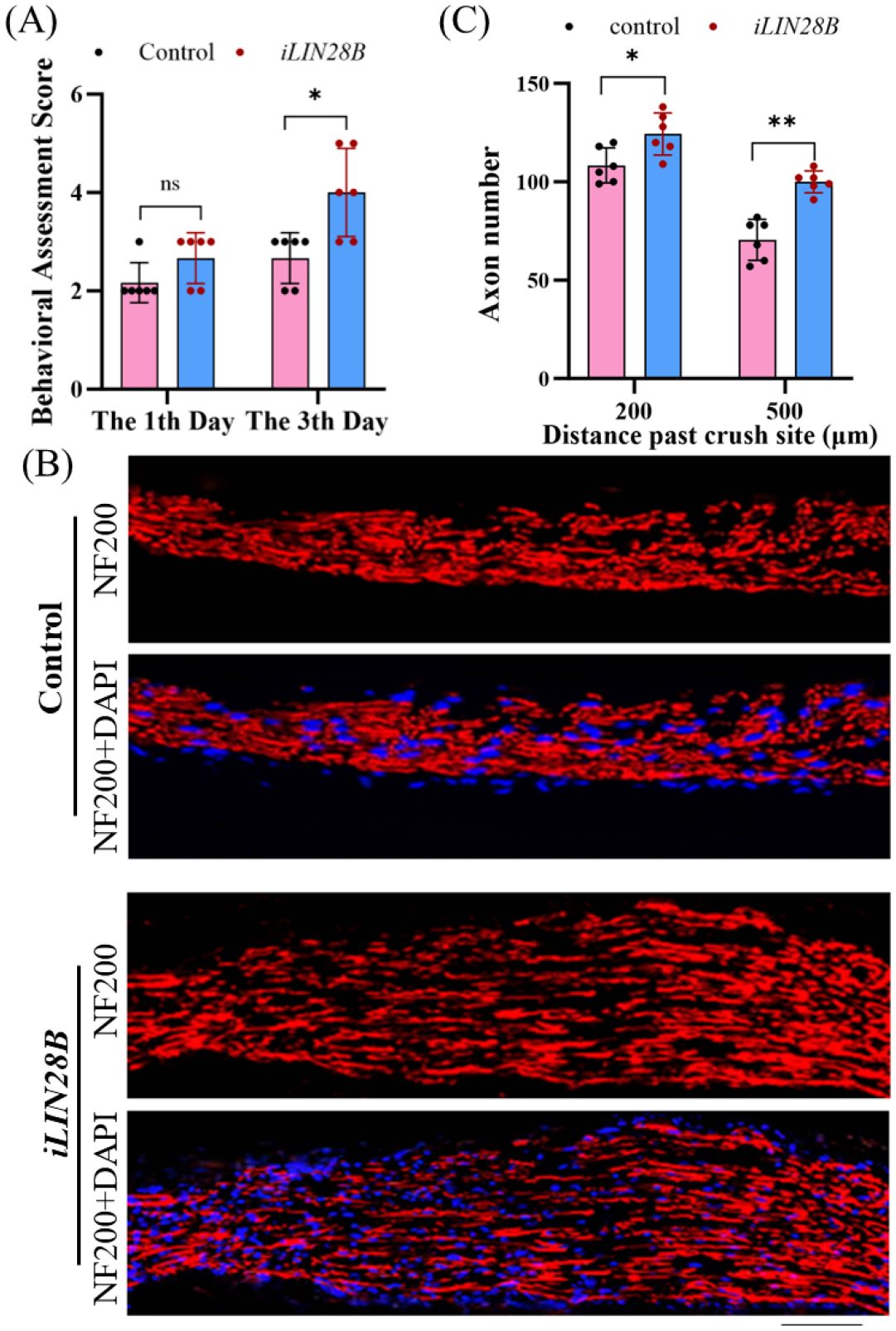

Fig. 4. Overexpression of Lin28b enhances motor functional recovery and axonal regeneration after facial nerve injury (FNI). (A) Facial nerve function scores were significantly higher in *iLIN28B* mice than in controls at 3 days post-FNI. (B) Immunofluorescence of facial nerve longitudinal sections (NF-200, axons) in control and *iLIN28B* mice at 3 days post-FNI (scale bar = 100 μm). (C) Statistical comparison of regenerating axon numbers in control and *iLIN28B* groups at 200 μm and 500 μm distal to the initial site of FNI. Group classification is based on the color of the individual data points in (A and C). Data are expressed as mean ± SEM. Unpaired two-tailed Student's *t*-tests; ns, not significant. $^{*}p < 0.05$, $^{**}p < 0.01$. n = 6 mice.

nificantly higher (124.33 ± 4.35) compared to the control group (108.33 ± 3.63; $p = 0.018$). At 500 µm distal to the injury site, the *iLIN28B* group maintained a higher axon count (100.00 ± 2.29), while the M2rtTA control group exhibited a marked reduction to 70.50 ± 4.25, resulting in an even more pronounced intergroup difference ($p < 0.01$) (Fig. 4B,C). These results demonstrate that overexpression of Lin28b effectively promotes functional recovery and enhances axonal regeneration following facial nerve injury.

To further validate the promotive effect of Lin28b overexpression in the brainstem facial nucleus on axonal regeneration, we isolated the facial nucleus from control and *iLIN28B* mice and established primary cultures of facial motor neurons. Lin28b expression was induced by adding doxycycline (dox) to the culture medium. After 3 days in culture, neurons from both control and *iLIN28B* groups exhibited clear somatic contours and extensive neurites, as shown in Fig. 5A. First, to investigate whether Lin28b overexpression affects cell viability, we quantified the number of neurons in the facial nucleus per mouse, averaged from three microscopic fields per animal. The results showed that the mean neuron count was 42.33 ± 1.62 in the control group and 45.00 ± 2.49 in the *iLIN28B* group, with no statistically significant difference between the two groups ($p = 0.406$; **Supplementary Fig. 1**). Subsequently, to quantitatively assess the effect of Lin28b overexpression on axon growth, we measured neurite length using immunofluorescence staining. The results (Fig. 5B,C) demonstrated that the maximum neurite length in the *iLIN28B* group was significantly greater than that in the control group (37.60 ± 1.67 µm vs. 25.10 ± 1.26 µm; $p = 0.003$). These findings indicate that Lin28b overexpression in facial motor neurons significantly promotes neurite outgrowth.

Lin28b Overexpression is Associated With Elevated Activation of Akt and S6 Kinases in the Primary Motor Cortex and Facial Nucleus

Given that rapamycin (an mTOR inhibitor) suppresses Lin28-mediated insulin sensitivity and enhances glucose uptake, while the insulin-PI3K/AKT/mTOR pathway is known to regulate let-7 function in non-neuronal mammalian cells [9], we further investigated whether upregulated Lin28b in the primary motor cortex and facial nucleus of *iLIN28B* mice with conditional Lin28b overexpression alters the activity of PI3K/AKT/mTOR pathway-associated kinases. Following normalization of target protein levels to the control group, Western blotting was used to measure the phosphorylation levels of Akt at Ser473 (pAkt) and ribosomal protein S6 at Ser235/236 (pS6), which reflect the activated states of Akt and S6 kinases, respectively. Compared to littermate control mice, *iLIN28B* mice exhibited significantly elevated pAkt levels in the primary motor cortex ($p < 0.001$) and facial motor nucleus ($p = 0.014$), while pS6 levels were significantly increased in the facial nucleus ($p = 0.009$) and showed a trend toward elevation in the primary motor cortex ($p = 0.020$) (Fig. 6). These findings suggest that Akt and S6 kinases may participate in regulating the role of Lin28 signaling within mouse motor neurons and facial nucleus neurons.

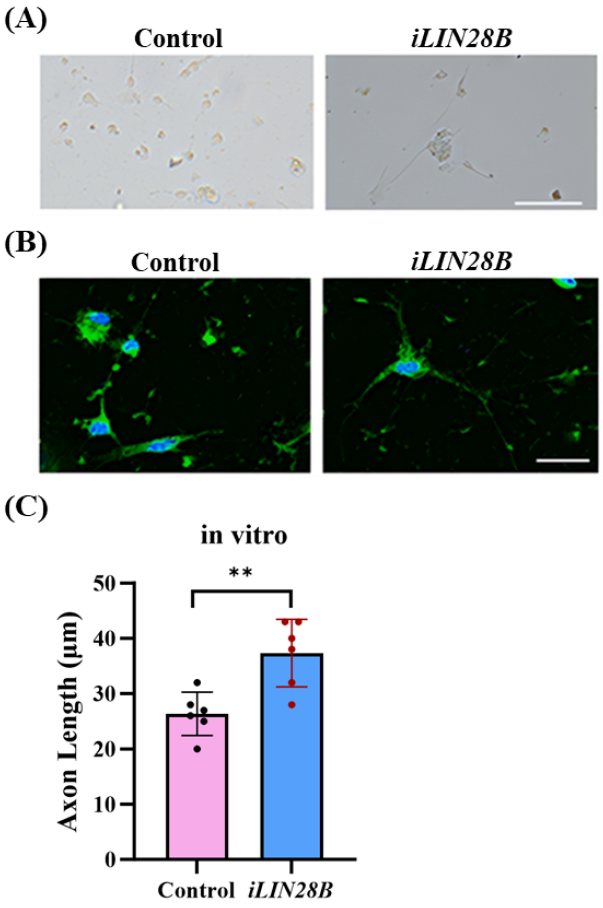

Fig. 5. Lin28b overexpression in the brainstem facial nucleus enhances neurite growth. (A) Primary neuronal cultures from the mouse facial nucleus after 3 days *in vitro*, showing the morphological appearance of control and *iLIN28B* groups. Scale bar = 100 µm. (B) β-Tubulin immunofluorescence of control and *iLIN28B* primary neurons from the facial nucleus at 3 days *in vitro*. Scale bar = 20 µm. (C) Quantification of neurite length in primary neurons from the mouse facial nucleus, showing a significant increase in the *iLIN28B* group compared to the control. Data are expressed as mean ± SEM. Unpaired two-tailed Student's *t*-tests. $^{**}p < 0.01$. n = 6 mice.

Discussion

This study uncovers dual regulatory roles of Lin28a/b in both developmental programming and injury-induced repair of the facial nerve. Using human LIN28B-inducible transgenic mice, we demonstrate that its conditional overexpression significantly enhances axonal regeneration and functional recovery post-facial

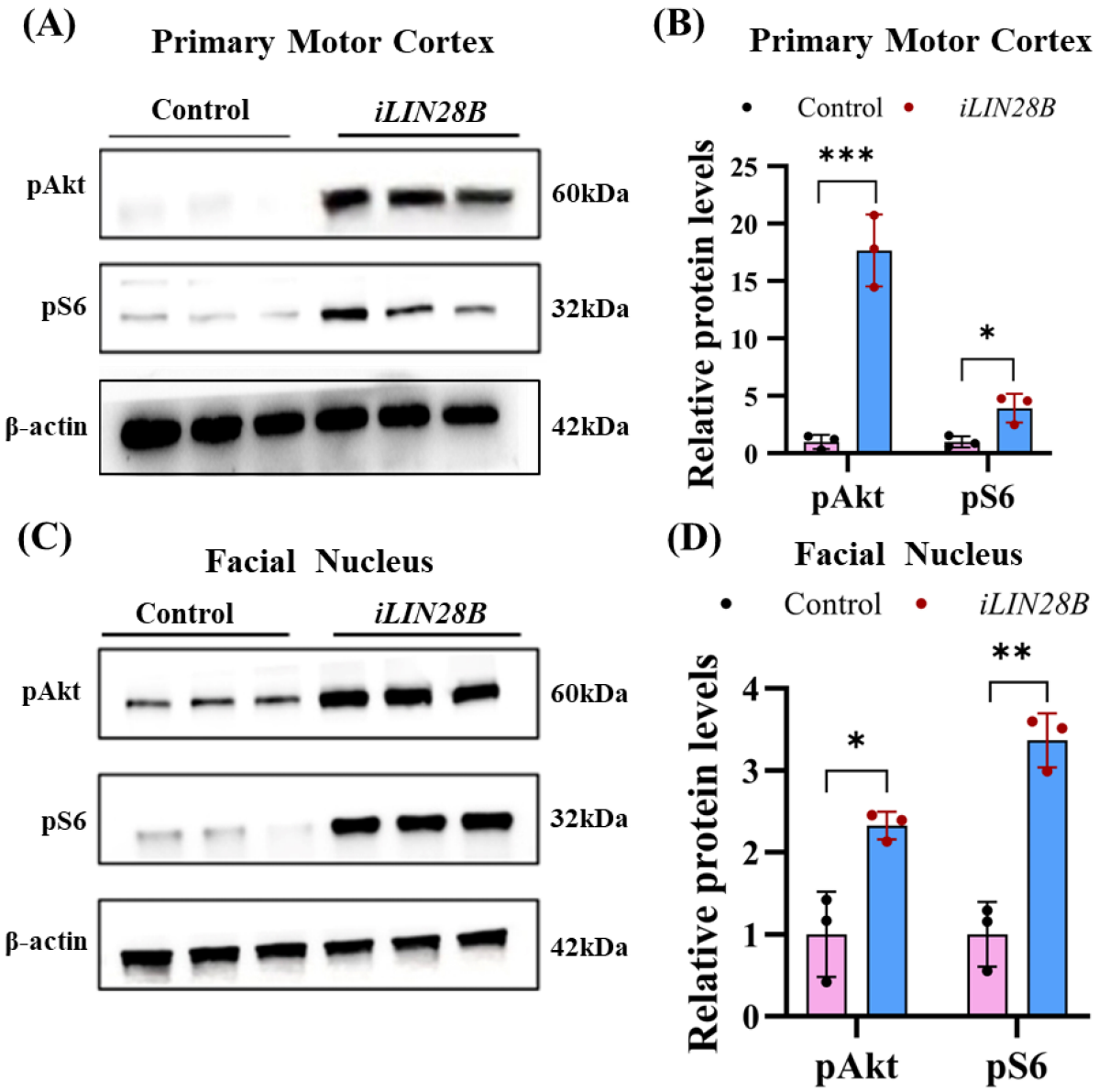

Fig. 6. Lin28b overexpression activates Akt and S6 kinases in the primary motor cortex and facial nucleus. (A) Representative Western blot results showed that Lin28b overexpression increased the levels of pAkt and pS6 in the primary motor cortex. (B) Quantification of (A). (C) Representative Western blot results showed that Lin28b overexpression increased the levels of pAkt and pS6 in the facial nucleus. (D) Quantification of (C) one sample *t*-test. Data are expressed as mean ± SEM. One sample *t*-test; $^{*}p < 0.05$, $^{**}p < 0.01$, $^{***}p < 0.001$, compared with the control if not designated. n = 3 independent experiments.

nerve injury, positioning Lin28b as a promising therapeutic target for motor nerve repair. As one of the few investigations elucidating the functional mechanisms of Lin28 in motor-dominant neural regeneration, this study significantly expands the current understanding of their regulatory networks within the peripheral nervous system.

The impaired regenerative capacity of adult mammalian nerves represents a complex biological challenge, in which the diminished intrinsic ability of mature neurons to sustain long-distance axonal growth serves as a critical limiting factor. Multiple signaling proteins, including mTOR, STAT3, c-Myc, and osteopontin, are critically involved in regulating neuronal survival and axonal regeneration processes in both the central nervous system and peripheral nervous system [24]. Therapeutic strategies targeting these genes to promote nervous system regeneration have been explored; however, even with combinatorial approaches, the overall regenerative outcomes achieved to date remain limited. In this study, we found that overexpression of Lin28b promotes motor function recovery and axonal regeneration following facial nerve injury. Combined with recent relevant studies [13,25], these findings collectively

substantiate the pivotal role of Lin28 in reprogramming multiple types of mature neurons in mammals. The absence of significant neuronal loss in the brainstem facial nucleus following peripheral facial nerve injury in adult mammals precludes rigorous assessment of Lin28-mediated neuroprotection, including critical anti-apoptotic mechanisms, in post-traumatic neuronal populations [26,27]. Previous research has identified biphasic properties in facial motor neurons of 2-week-old mice: these neurons retain hallmark features of mature motor neurons while also exhibiting responsiveness to peripheral facial nerve injury, with neuronal apoptosis rates reaching approximately 20% [28]. Based on these findings, the present study employed a facial nerve crush injury model in 2-week-old mice to systematically investigate the regulatory mechanisms of Lin28 in axonal regeneration following neural injury.

Lin28, an RNA-binding protein initially discovered in *Caenorhabditis elegans*, regulates the temporal progression of developmental events [29], including the specification of late-stage cell fates and terminal differentiation of specific cell types [30–32]. Lin28 plays a pivotal role in mediating the transition of pluripotent stem cells to committed cell lineages [33], and it enables the reprogramming of mammalian somatic cells into pluripotent cells by promoting their cell division [34,35]. Previous research has demonstrated that Lin28 is essential for controlling the proliferation of neural precursor cells *in vitro* and also in the developing brain [36]. This study revealed that during neural system development, the expression patterns of Lin28a/b in the primary motor cortex and brainstem facial nucleus exhibit spatiotemporal concordance with previously documented profiles in embryonic forebrain tissues and dorsal root ganglia (Fig. 1) [22,37]. The evolutionary conservation of these trans-neuroanatomical spatiotemporal expression patterns further elucidates Lin28's precise temporal regulation of developmental timing during neural system ontogeny.

Lin28 regulates cell growth through dual pathways that are both let-7-dependent and let-7-independent [38]. In nematodes and mammals, the most canonical mechanism of Lin28 involves modulating let-7 activity to exert its biological functions [39]. In *Caenorhabditis elegans*, let-7 has been demonstrated to suppress regeneration of anteroventral microtubule neurons [40]. However, skeletal muscle-specific knockout of Lin28 in mice elicited impaired glucose tolerance and insulin resistance without altering let-7 expression levels [9]. Research using transgenic mouse models has demonstrated that inhibition of let-7 is a necessary but not sufficient condition for tissue repair [7]. For example, in the peripheral nervous system model, following sciatic nerve crush injury, enhanced let-7 activity not only suppresses axonal regeneration of sensory neurons in the spinal dorsal root ganglia but also completely abolishes the accelerated regeneration induced by Lin28b overexpression. Conversely, loss of let-7 function significantly promotes the regenerative process [22]. However, in the optic nerve injury model of the central nervous system, although Lin28a overexpression significantly promotes axonal regeneration, whether its effect depends on the let-7 pathway remains unclear [14]. This study revealed that facial nerve injury induces upregulation of endogenous Lin28a/b mRNA levels in the brainstem facial motor nucleus (Fig. 2A,B), accompanied by a concomitant downregulation of let-7 miRNAs (Fig. 2C,D). Notably, the temporal upregulation of Lin28a/b mRNA precedes the decline in let-7 miRNA levels (Fig. 2E,F). The temporal dynamics of the Lin28/let-7 axis within the facial motor nucleus suggest its pivotal role in orchestrating the repair process following facial nerve injury through dynamic regulation of axon regeneration-associated genes. In *iLIN28B* mice with Lin28b overexpression, the LIN28B protein levels in the facial nerve nucleus were significantly increased, accompanied by a widespread downregulation of the let-7 miRNA family (Fig. 3B,C). Immunofluorescence analysis further revealed that the *iLIN28B* group maintained a relatively higher number of axons at 500 μm distal to the injury site, which was significantly greater than that of the control group. In contrast, the control group exhibited a sharp decrease in axonal number from 200 μm to 500 μm (Fig. 4B,C). Although Lin28A and Lin28B belong to the same protein family and both suppress let-7 biogenesis, they exhibit distinct molecular mechanisms and tissue-specific functions [41–43]. Lin28A primarily functions in the cytoplasm and is predominantly expressed during early embryonic development, whereas Lin28B contains a nuclear localization signal, acts in the nucleus, and shows broader and more sustained expression [44,45]. Importantly, previous studies have indicated that Lin28A is mainly involved in axonal regeneration following central nervous system injury [46,47], whereas Lin28B plays a predominant role in peripheral nerve regeneration [22]. Given that the facial nerve is part of the peripheral nervous system, we chose to focus on Lin28B for *in vivo* experiments in this study. Additionally, as shown in Fig. 5, primary neurons from the brainstem facial nucleus cultured for 3 days *in vitro* in the *iLIN28B* group demonstrated a significant increase in neurite length compared to the control group. These results collectively indicate that overexpression of Lin28b in the facial nucleus enhances axonal regenerative capacity by suppressing let-7 biogenesis. These findings suggest that the direct regulatory relationship between Lin28 and let-7, which is well-established in the peripheral nervous system, may be modulated by additional molecular pathways or partially replaced in the central nervous system. These discrepancies indicate that the molecular mechanisms underlying Lin28-mediated axonal regeneration likely exhibit region-specific features within the nervous system.

The signaling pathways through which Lin28 regulates the axonal growth of neurons in the mature central and peripheral nervous systems remain poorly elucidated. Pre-

vious research has established that Lin28/let-7 modulates glucose metabolism via the insulin-phosphatidylinositol 3-kinase (PI3K)-Akt signaling pathway [9]. We examined the activity of the PI3K-mTOR pathway in *iLIN28B* mice. Western blotting results showed that compared with the control group, the phosphorylation levels of Akt (Ser473) and S6 ribosomal protein (Ser235/236) (pAkt, pS6) were significantly increased in the primary motor cortex and facial nucleus of *iLIN28B* mice (Fig. 6). As an RNA-binding protein, Lin28 markedly enhances the translation efficiency of a broad spectrum of mRNAs, including IGF-PI3K-mTOR pathway genes and cell cycle regulatory genes (e.g., *Myc*, *Ras*, *Hmga2*), by suppressing let-7 [48,49]. Specifically, upon activation of PI3K by Lin28, phosphorylated Akt targets the tuberous sclerosis complex (TSC1/2, a GTPase-activating protein), thereby activating the mTOR pathway to promote S6 kinase phosphorylation and regulate neuronal growth [50]. Studies have demonstrated that Lin28 signaling interacts with the extracellular signal-regulated kinase (ERK) and AMP-activated protein kinase (AMPK) pathways in stem cells and cancer cells [51,52]. Recent studies have further demonstrated that Lin28 overexpression significantly upregulates the levels of Thr202/Tyr204-phosphorylated p44/42 MAPK (p-Erk) and Thr172-phosphorylated AMPKα (p-AMPKα) in the sensorimotor cortex [14,53]. Notably, targeting the PI3K/mTOR or ERK pathways has been demonstrated to promote central neuron regeneration [53,54], while AMPK regulates axon initiation and neuronal polarization during development [55]. Collectively, these findings suggest that Lin28 may promote neuronal growth and regeneration by synergistically activating the Akt-mTOR, ERK, and AMPK pathways.

Conclusions

This study reveals that Lin28a/b has dual regulatory roles in facial nerve development and injury repair. Lin28a/b shows dynamic expression during nerve development and is upregulated after facial nerve injury, acting upstream of let-7 miRNAs to promote axonal regeneration. Overexpressing Lin28b in transgenic mice suppresses let-7 miRNA levels, enhances facial nerve functional recovery and axon regeneration. Mechanistically, the pro-regenerative effect of Lin28 overexpression may be partially mediated by the PI3K-AKT-mTOR pathway. These findings identify Lin28b as a potential therapeutic target for motor nerve repair, leveraging its dual role in RNA metabolism and growth pathway activation.

Availability of Data and Materials

The data that support the findings of this study are available from the corresponding author upon reasonable request.

Author Contributions

XYG: Writing - original draft, Methodology, Formal analysis, Data acquisition and curation, Conceptualization; QH: Writing - original draft, Data acquisition, Supervision, Methodology, Conceptualization; QL: Writing - review & editing, Data curation, Supervision, Conceptualization; KL: Writing - review & editing, Acquisition and collation of experimental data, Resources; SMY: Writing - review & editing, Supervision, Resources, Conceptualization; WDS: Writing - review & editing, Methodology, Formal analysis, Supervision, Resources, Conceptualization. All authors have read and agreed to the published version of the manuscript. All authors have participated sufficiently in the work to take public responsibility for appropriate portions of the content and agreed to be accountable for all aspects of the work in ensuring that questions related to its accuracy or integrity.

Ethics Approval and Consent to Participate

All animal procedures were approved by the Animal Ethics Committee of the Chinese PLA General Hospital (Approval No.2020-X16-50). All animal experiments in this study were performed in strict accordance with the ARRIVE Guideline 2.0 and the institutional animal care and use guidelines.

Acknowledgment

We thank Professor Xiaojun Li's laboratory at Xi'an Jiaotong University for generously providing the transgenic mice. We also thank all participants for their cooperation.

Funding

This study was supported by the National Key Research and Development Program of China (Grant Nos. 2022YFC2402704 and 2022YFC2402705).

Conflict of Interest

The authors declare no conflict of interest.

Supplementary Material

Supplementary material associated with this article can be found, in the online version, at https://doi.org/10.24976/Discov.Med.202638209.139.

References

[1] Kim SJ, Lee HY. Acute Peripheral Facial Palsy: Recent Guidelines and a Systematic Review of the Literature. Journal of Korean Medical Science. 2020; 35: e245. https://doi.org/10.3346/jkms.2020.35.e245.

[2] Kim SH, Jung J, Jung SY, Dong SH, Byun JY, Park MS, *et al*. Comparative prognosis in patients with Ramsay-Hunt

syndrome and Bell's palsy. European Archives of Oto-rhino-laryngology: Official Journal of the European Federation of Oto-Rhino-Laryngological Societies (EUFOS): Affiliated with the German Society for Oto-Rhino-Laryngology - Head and Neck Surgery. 2019; 276: 1011–1016. https://doi.org/10.1007/s00405-019-05300-3.

[3] Leong SC, Lesser TH. A national survey of facial paralysis on the quality of life of patients with acoustic neuroma. Otology & neurotology: official publication of the American Otological Society, American Neurotology Society [and] European Academy of Otology and Neurotology. 2015; 36: 503–509. https://doi.org/10.1097/MAO.0000000000000428.

[4] Mahar M, Cavalli V. Intrinsic mechanisms of neuronal axon regeneration. Nature Reviews. Neuroscience. 2018; 19: 323–337. https://doi.org/10.1038/s41583-018-0001-8.

[5] Galvao J, Iwao K, Apara A, Wang Y, Ashouri M, Shah TN, *et al*. The Krüppel-Like Factor Gene Target Dusp14 Regulates Axon Growth and Regeneration. Investigative Ophthalmology & Visual Science. 2018; 59: 2736–2747. https://doi.org/10.1167/iovs.17-23319.

[6] Nandan MO, Yang VW. The role of Krüppel-like factors in the reprogramming of somatic cells to induced pluripotent stem cells. Histology and Histopathology. 2009; 24: 1343–1355. https://doi.org/10.14670/HH-24.1343.

[7] Yu J, Vodyanik MA, Smuga-Otto K, Antosiewicz-Bourget J, Frane JL, Tian S, *et al*. Induced pluripotent stem cell lines derived from human somatic cells. Science (New York, N.Y.). 2007; 318: 1917–1920. https://doi.org/10.1126/science.1151526.

[8] Shinoda G, Shyh-Chang N, Soysa TYD, Zhu H, Seligson MT, Shah SP, *et al*. Fetal deficiency of lin28 programs life-long aberrations in growth and glucose metabolism. Stem Cells (Dayton, Ohio). 2013; 31: 1563–1573. https://doi.org/10.1002/stem.1423.

[9] Zhu H, Shyh-Chang N, Segrè AV, Shinoda G, Shah SP, Einhorn WS, *et al*. The Lin28/let-7 axis regulates glucose metabolism. Cell. 2011; 147: 81–94. https://doi.org/10.1016/j.cell.2011.08.033.

[10] Ramachandran R, Fausett BV, Goldman D. Ascl1a regulates Müller glia dedifferentiation and retinal regeneration through a Lin-28-dependent, let-7 microRNA signalling pathway. Nature Cell Biology. 2010; 12: 1101–1107. https://doi.org/10.1038/ncb2115.

[11] Heo I, Joo C, Cho J, Ha M, Han J, Kim VN. Lin28 mediates the terminal uridylation of let-7 precursor MicroRNA. Molecular Cell. 2008; 32: 276–284. https://doi.org/10.1016/j.molcel.2008.09.014.

[12] Vadla B, Kemper K, Alaimo J, Heine C, Moss EG. lin-28 controls the succession of cell fate choices via two distinct activities. PLoS Genetics. 2012; 8: e1002588. https://doi.org/10.1371/journal.pgen.1002588.

[13] Zhang Q, Tang JH, Liu LY, Liu Z, Xue JF, Ge J, *et al*. Emerging therapeutic strategies for optic nerve regeneration. Trends in Pharmacological Sciences. 2025; 46: 128–142. https://doi.org/10.1016/j.tips.2024.11.008.

[14] Nathan FM, Ohtake Y, Wang S, Jiang X, Sami A, Guo H, *et al*. Upregulating Lin28a Promotes Axon Regeneration in Adult Mice with Optic Nerve and Spinal Cord Injury. Molecular Therapy: the Journal of the American Society of Gene Therapy. 2020; 28: 1902–1917. https://doi.org/10.1016/j.ymthe.2020.04.010.

[15] Zhang X, Duan X, Liu X. The role of kinases in peripheral nerve regeneration: mechanisms and implications. Frontiers in Neurology. 2024; 15: 1340845. https://doi.org/10.3389/fneur.2024.1340845.

[16] Shan F, Yao X, Zhang Q, Li R, Kong L, Zheng Q, *et al*. NMDA Receptors Coordinate Metabolic Reprogramming and Mitophagy in Schwann Cells to Promote Peripheral Nerve Regeneration. Research (Washington, D.C.). 2025; 8: 0825. https://doi.org/10.34133/research.0825.

[17] Gencel-Augusto J, Grandis JR, Johnson DE. Conventional and alternative approaches for targeting PIK3CA and PTEN alterations in head and neck, breast, and other cancers. Advances in Biological Regulation. 2026; 99: 101117. https://doi.org/10.1016/j.jbior.2025.101117.

[18] Thakkar V, Mehdipour M, Chang S. Unlocking nerve regeneration: electrical stimulation and bioscaffolds to enhance peripheral nerve regeneration. Frontiers in Neuroscience. 2025; 19: 1594435. https://doi.org/10.3389/fnins.2025.1594435.

[19] Fei J, Chen S, Song X, Liang Y, Duan K, Peng X, *et al*. Exogenous GDNF promotes peripheral facial nerve regeneration in rats through the PI3K/AKT/mTOR signaling pathway. FASEB Journal: Official Publication of the Federation of American Societies for Experimental Biology. 2024; 38: e23340. https://doi.org/10.1096/fj.202301664R.

[20] Ishii A, Furusho M, Bansal R. Mek/ERK1/2-MAPK and PI3K/Akt/mTOR signaling plays both independent and cooperative roles in Schwann cell differentiation, myelination and dysmyelination. Glia. 2021; 69: 2429–2446. https://doi.org/10.1002/glia.24049.

[21] Wu L, Zhang Z, Tian D, Chen K, Liang JH, Yu H, *et al*. Hirudin promotes peripheral nerve repair and alleviates pain by regulating the EGFR-PI3K/AKT/mTOR pathway. Archives of Biochemistry and Biophysics. 2026; 775: 110671. https://doi.org/10.1016/j.abb.2025.110671.

[22] Wang XW, Li Q, Liu CM, Hall PA, Jiang JJ, Katchis CD, *et al*. Lin28 Signaling Supports Mammalian PNS and CNS Axon Regeneration. Cell Reports. 2018; 24: 2540–2552.e6. https://doi.org/10.1016/j.celrep.2018.07.105.

[23] de Faria SD, Testa JRG, Borin A, Toledo RN. Standardization of techniques used in facial nerve section and facial movement evaluation in rats. Brazilian Journal of Otorhinolaryngology. 2006; 72: 341–347. https://doi.org/10.1016/s1808-8694(15)30966-6.

[24] Belin S, Nawabi H, Wang C, Tang S, Latremoliere A, Warren P, *et al*. Injury-induced decline of intrinsic regenerative ability revealed by quantitative proteomics. Neuron. 2015; 86: 1000–1014. https://doi.org/10.1016/j.neuron.2015.03.060.

[25] Zhang Y, Williams PR, Jacobi A, Wang C, Goel A, Hirano AA, *et al*. Elevating Growth Factor Responsiveness and Axon Regeneration by Modulating Presynaptic Inputs. Neuron. 2019; 103: 39–51.e5. https://doi.org/10.1016/j.neuron.2019.04.033.

[26] Wang S, Li S. Lin28 as a therapeutic target for central nervous system regeneration and repair. Neural Regeneration Research. 2024; 19: 397–398. https://doi.org/10.4103/1673-5374.375322.

[27] Dai W, Li Y, Du J, Shen G, Fan M, Su Z, *et al*. Transplanting neural stem cells overexpressing miRNA-21 can promote neural recovery after cerebral hemorrhage through the SOX2/LIN28-let-7 signaling pathway. Animal Models and Experimental Medicine. 2025; 8: 1760–1774. https://doi.org/10.1002/ame2.70009.

[28] Nakajima K, Ishijima T. Events Occurring in the Axotomized Facial Nucleus. Cells. 2022; 11: 2068. https://doi.org/10.3390/cells11132068.

[29] Moss EG, Lee RC, Ambros V. The cold shock domain protein LIN-28 controls developmental timing in C. elegans and is regulated by the lin-4 RNA. Cell. 1997; 88: 637–646. https://doi.org/10.1016/s0092-8674(00)81906-6.

[30] Tsialikas J, Romer-Seibert J. LIN28: roles and regulation in development and beyond. Development (Cambridge, England). 2015; 142: 2397–2404. https://doi.org/10.1242/dev.117580.

[31] Thevarajan I, Osuna MF, Lewey SF, Sauceda E, Briseno S, Grif-

fin C, *et al*. LIN28-mediated gene regulatory loops synchronize transitions throughout organogenesis. Biochemistry and Biophysics Reports. 2025; 44: 102226. https://doi.org/10.1016/j.bbrep.2025.102226.

[32] Navolić J, Hawass S, Moritz M, Hahn J, Middelkamp M, Gocke A, *et al*. Spatial Proteomics Reveals Distinct Protein Patterns in Cortical Migration Disorders Caused by LIN28A Overexpression and WNT Activation. Molecular & Cellular Proteomics: MCP. 2025; 24: 101037. https://doi.org/10.1016/j.mcpro.2025.101037.

[33] Faas L, Warrander FC, Maguire R, Ramsbottom SA, Quinn D, Genever P, *et al*. Lin28 proteins are required for germ layer specification in Xenopus. Development (Cambridge, England). 2013; 140: 976–986. https://doi.org/10.1242/dev.089797.

[34] Hanna J, Saha K, Pando B, van Zon J, Lengner CJ, Creyghton MP, *et al*. Direct cell reprogramming is a stochastic process amenable to acceleration. Nature. 2009; 462: 595–601. https://doi.org/10.1038/nature08592.

[35] Pieknell K, Sulistio YA, Wulansari N, Darsono WHW, Chang MY, Ko JY, *et al*. LIN28A enhances regenerative capacity of human somatic tissue stem cells via metabolic and mitochondrial reprogramming. Cell Death and Differentiation. 2022; 29: 540–555. https://doi.org/10.1038/s41418-021-00873-1.

[36] Yang M, Yang SL, Herrlinger S, Liang C, Dzieciatkowska M, Hansen KC, *et al*. Lin28 promotes the proliferative capacity of neural progenitor cells in brain development. Development (Cambridge, England). 2015; 142: 1616–1627. https://doi.org/10.1242/dev.120543.

[37] Morgado AL, Rodrigues CMP, Solá S. MicroRNA-145 Regulates Neural Stem Cell Differentiation Through the Sox2-Lin28/let-7 Signaling Pathway. Stem Cells (Dayton, Ohio). 2016; 34: 1386–1395. https://doi.org/10.1002/stem.2309.

[38] Nam Y, Chen C, Gregory RI, Chou JJ, Sliz P. Molecular basis for interaction of let-7 microRNAs with Lin28. Cell. 2011; 147: 1080–1091. https://doi.org/10.1016/j.cell.2011.10.020.

[39] Hagan JP, Piskounova E, Gregory RI. Lin28 recruits the TUTase Zcchc11 to inhibit let-7 maturation in mouse embryonic stem cells. Nature Structural & Molecular Biology. 2009; 16: 1021–1025. https://doi.org/10.1038/nsmb.1676.

[40] Zou Y, Chiu H, Zinovyeva A, Ambros V, Chuang CF, Chang C. Developmental decline in neuronal regeneration by the progressive change of two intrinsic timers. Science (New York, N.Y.). 2013; 340: 372–376. https://doi.org/10.1126/science.1231321.

[41] Cotino-Nájera S, García-Villa E, Cruz-Rosales S, Gariglio P, Díaz-Chávez J. The role of Lin28A and Lin28B in cancer beyond Let-7. FEBS Letters. 2024; 598: 2963–2979. https://doi.org/10.1002/1873-3468.15004.

[42] Hao Z, Wu Y, Huang Y, Zhang M, Liu Y, Li Y, *et al*. Microprotein PLUM encoded by Lin28b uORF is a cytoplasmic determinant of pluripotency and embryonic development. Nature Communications. 2025; 16: 10324. https://doi.org/10.1038/s41467-025-66297-4.

[43] Oyejobi GK, Yan X, Sliz P, Wang L. Regulating Protein-RNA Interactions: Advances in Targeting the LIN28/Let-7 Pathway. International Journal of Molecular Sciences. 2024; 25: 3585. https://doi.org/10.3390/ijms25073585.

[44] Krsnik D, Marić T, Bulić-Jakuš F, Sinčić N, Bojanac AK. LIN28 Family in Testis: Control of Cell Renewal, Maturation, Fertility and Aging. International Journal of Molecular Sciences. 2022; 23: 7245. https://doi.org/10.3390/ijms23137245.

[45] Maklad A, Sedeeq M, Chan KM, Gueven N, Azimi I. Exploring Lin28 proteins: Unravelling structure and functions with emphasis on nervous system malignancies. Life Sciences. 2023; 335: 122275. https://doi.org/10.1016/j.lfs.2023.122275.

[46] Hu Z, Ma J, Yue H, Luo Y, Li X, Wang C, *et al*. Involvement of LIN28A in Wnt-dependent regulation of hippocampal neurogenesis in the aging brain. Stem Cell Reports. 2022; 17: 1666–1682. https://doi.org/10.1016/j.stemcr.2022.05.016.

[47] Hu Z, Ma J, Gu Y. Lin28a is Essential for Synaptic Plasticity in Dentate Granule Cells and Spatial Memory. Neuroscience Bulletin. 2021; 37: 261–266. https://doi.org/10.1007/s12264-020-00591-7.

[48] Shaik Syed Ali P, Ahmad MP, Parveen KMH. Lin28/let-7 axis in breast cancer. Molecular Biology Reports. 2025; 52: 311. https://doi.org/10.1007/s11033-025-10413-6.

[49] Wang X, Van PKT, Liu B, Zhao T, Wu YS. Targeting the Lin28/let-7 Axis with Compounds to Regulate Transcriptional Control in Cancer. Anti-cancer Agents in Medicinal Chemistry. 2026; 26: 121–136. https://doi.org/10.2174/0118715206375441250901064006.

[50] Patel S, Prajapati C, Rai SN, Singh SK. Bridging pathway dysfunction and therapy: novel compounds for neuroprotection. 3 Biotech. 2026; 16: 79. https://doi.org/10.1007/s13205-026-04697-z.

[51] Zhao Y, Liu Y, Lin L, Huang Q, He W, Zhang S, *et al*. The lncRNA MACC1-AS1 promotes gastric cancer cell metabolic plasticity via AMPK/Lin28 mediated mRNA stability of MACC1. Molecular Cancer. 2018; 17: 69. https://doi.org/10.1186/s12943-018-0820-2.

[52] Liu X, Chen M, Li L, Gong L, Zhou H, Gao D. Extracellular Signal-regulated Kinases (ERKs) Phosphorylate Lin28a Protein to Modulate P19 Cell Proliferation and Differentiation. The Journal of Biological Chemistry. 2017; 292: 3970–3976. https://doi.org/10.1074/jbc.C117.775122.

[53] Akram R, Anwar H, Javed MS, Rasul A, Imran A, Malik SA, *et al*. Axonal Regeneration: Underlying Molecular Mechanisms and Potential Therapeutic Targets. Biomedicines. 2022; 10: 3186. https://doi.org/10.3390/biomedicines10123186.

[54] Nieuwenhuis B, Eva R. Promoting axon regeneration in the central nervous system by increasing PI3-kinase signaling. Neural Regeneration Research. 2022; 17: 1172–1182. https://doi.org/10.1016/j.semcdb.2022.02.011.

[55] Li MX, Weng JW, Ho ES, Chow SF, Tsang CK. Brain delivering RNA-based therapeutic strategies by targeting mTOR pathway for axon regeneration after central nervous system injury. Neural Regeneration Research. 2022; 17: 2157–2165. https://doi.org/10.4103/1673-5374.335830.